Efficient estimation of decay parameters in acoustically coupled-spaces using slice sampling[a)]

Tomislav Jasa
Thalgorithm Research, Toronto, Ontario L4X 1B1, Canada

Ning Xiang[b)]
Graduate Program in Architectural Acoustics, School of Architecture, Rensselaer Polytechnic Institute, Troy, New York 12180

(Received 1 September 2008; revised 27 May 2009; accepted 30 May 2009)

Room-acoustic energy decay analysis of acoustically coupled-spaces within the Bayesian framework has proven valuable for architectural acoustics applications. This paper describes an efficient algorithm termed slice sampling Monte Carlo (SSMC) for room-acoustic decay parameter estimation within the Bayesian framework. This work combines the SSMC algorithm and a fast search algorithm in order to efficiently determine decay parameters, their uncertainties, and inter-relationships with a minimum amount of required user tuning and interaction. The large variations in the posterior probability density functions over multidimensional parameter spaces imply that an adaptive exploration algorithm such as SSMC can have advantages over the exiting importance sampling Monte Carlo and Metropolis–Hastings Markov Chain Monte Carlo algorithms. This paper discusses implementation of the SSMC algorithm, its initialization, and convergence using experimental data measured from acoustically coupled-spaces.
© *2009 Acoustical Society of America.* [DOI: 10.1121/1.3158934]

PACS number(s): 43.60.Uv, 43.60.Jn, 43.55.Mc [EJS] Pages: 1269–1279

I. INTRODUCTION

Bayesian probabilistic inference has been increasingly applied in acoustics applications ranging from architectural acoustics,[1,2] geo-acoustic inversion, source tracking,[3–6] and underwater acoustics applications.[7–9] The Bayesian formalism specifically applied to decay time evaluation in acoustically coupled-spaces has proven to be a useful framework for analyzing Schroeder decay functions[10] from room impulse response measurements. This framework allows one to estimate not only the decay parameters from the Schroeder decay model,[1] but also to determine the decay order,[2] quantify uncertainties of decay estimates, and determine the inter-relationship between multiple decay parameters.[11] Due to computational demands, it is common to use Markov chain Monte Carlo (MCMC) and Monte Carlo (MC) algorithms such as importance sampling Monte Carlo (ISMC) integration[3,6,11] for numerical calculation within the Bayesian framework. ISMC integration and MCMC algorithms represent effective approaches to estimate the decay parameters, quantify the estimate uncertainties, and determine decay inter-relationships in cases where it is possible to properly initialize these algorithms. Using an analytic example and sample posterior probability density functions (PPDFs) of acoustically coupled rooms, this paper discusses the difficulty in choosing a good ISMC sampling or MCMC proposal distributions, which often require significant user effort. A deterministic fast search (FS) algorithm,[12] which is less dependent on user initialization, is only able to estimate decay parameters; however, it cannot quantify uncertainties in the estimates nor can it determine inter-relationships between decay parameters. For data analysis, the uncertainties and inter-relationships of relevant parameters are of as the same importance as the parameters themselves.

This paper describes an efficient algorithm termed slice sampling Monte Carlo (SSMC), recently introduced by Neal,[13] as a generic sampling method. The paper shows how the SSMC algorithm combined with the FS algorithm[12] can be applied to Bayesian analysis of acoustically coupled-spaces. The SSMC algorithm has not yet been documented (at least to the best knowledge of the authors) in acoustic applications. As Bayesian inferential methods have increasingly found applications in acoustics research, the introduction of the SSMC algorithm in the context of architectural acoustics may also benefit acousticians who are working on Bayesian methods in other acoustics applications. Specifically, the significance of this work for architectural acousticians is that an increased accuracy, higher efficiency, and critically less user-interaction within the Bayesian framework can be achieved for sound energy decay analysis, particularly for multiple-slope decays, often encountered in acoustically coupled-spaces.[14–17] High efficiency is required in practice, since architectural acousticians often need to analyze multiple decay times and related parameters, along with their uncertainties over 6–8 octave bands or over 10–22 third-octave bands. Reducing the required user tuning and interaction is beneficial to acousticians who are unaccustomed with ISMC and MCMC algorithms but who still

[a)] Aspects of this work have been presented at the 152nd ASA Meeting in Honolulu 2006 and at the 155th ASA Meeting in Paris.
[b)] Author to whom correspondence should be addressed. Electronic mail: xiangn@rpi.edu

require the benefits of Bayesian analysis.

This paper is organized as follows, Sec. II briefly describes Bayesian formulation of a PPDF over the decay parameter space. Section III discusses the difficulties in choosing an appropriate ISMC sampling distribution and the related problem in choosing an appropriate proposal distribution in MCMC algorithms (focusing on the commonly used Metropolis–Hastings algorithm). Section IV discusses implementation aspects of the SSMC algorithm used in this work. Section V shows the results of the SSMC/FS algorithm applied to experimentally obtained Schroeder decay functions. Section VI concludes the paper.

II. BAYESIAN FORMULATION

A detailed explanation in the Bayesian framework is given in the papers by Xiang and Jasa;[12] this paper begins with a brief review on the Schroeder decay function model for determining the decay parameters in acoustically coupled-spaces. A linear parametric model **GA** approximates the experimental data **D** as follows:

$$\mathbf{D} = \mathbf{GA} + \mathbf{e}, \tag{1}$$

with an error **e** where **A** is a vector of m weighting coefficients and **G** is a $K \times m$ discretized model matrix, with the jth column of **G** given by

$$G_{kj}(T_j, t_k) = \begin{cases} t_K - t_k & \text{for } j = 0 \\ \exp(-13.8 t_k / T_j) & \text{for } j = 1,2,\ldots,m-1. \end{cases} \tag{2}$$

T_j in Eq. (2) is the jth decay time parameter to be determined for $0 \le j \le m-1$, $T_0 = \infty$, $0 \le k \le K-1$, and t_K represents the upper limit of Schroeder's integration and K is the number of data points of the Schroeder decay function. The validity of this model for determining the decay times in acoustically coupled-spaces has been experimentally verified (especially when t_K is large) in Ref. 11. This work applies a Bayesian analysis to the decay model in Eq. (1) as briefly summarized below. Prior to analysis, the error components e_i are only known to be of a finite amount of energy. With this being the only information I available, the application of the principle of maximum entropy[18] leads to assignment of a likelihood function

$$l(\mathbf{T}, \mathbf{A}, \sigma | \mathbf{D}, I) = (\sqrt{2\pi}\sigma)^{-K} \exp\left(\frac{-\mathbf{e}^{\mathrm{Tr}}\mathbf{e}}{2\sigma^2} \right), \tag{3}$$

where **T** is the vector of the decay times and **A** is a vector of linear coefficients and Tr denotes a matrix transpose. Both **A** and **T** are decay parameters that the authors wish to find. The parameter σ^2 in Eq. (3) represents a finite but unspecified error variance. In room-acoustics practice, acousticians are challenged to estimate decay parameters for multiple-sloped sound energy decays. For a double-sloped decay [$m=3$ in Eq. (2)] this results in a likelihood function over a six-dimensional parameter space, with σ being one additional parameter along with three linear (A_j) and two (nonlinear) decay time (T_j) parameters. At this point it is possible to marginalize over the error variance leaving the likelihood in terms of the decay times and the linear coefficients as shown in Appendix A. This results in a likelihood function in the form of a student-T distribution

$$l(\mathbf{T}, \mathbf{A} | \mathbf{D}, I) = (2\pi)^{-K/2} \Gamma\left(\frac{K}{2} \right) \frac{Q^{-K/2}}{2} \tag{4}$$

with

$$Q = \frac{\mathbf{e}^{\mathrm{Tr}}\mathbf{e}}{2} \tag{5}$$

and gamma function $\Gamma(x)$.

The PPDF of $\mathbf{T}, \mathbf{A}$ given data **D** and the available background information I as noted by $p(\mathbf{T}, \mathbf{A} | \mathbf{D}, I)$ are defined by the likelihood and prior probability $\pi(\mathbf{T}, \mathbf{A} | I)$ of the decay parameters

$$p(\mathbf{T}, \mathbf{A} | \mathbf{D}, I) = \frac{1}{Z} l(\mathbf{T}, \mathbf{A} | \mathbf{D}, I) \pi(\mathbf{T}, \mathbf{A} | I), \tag{6}$$

where

$$Z = \int l(\mathbf{T}, \mathbf{A} | \mathbf{D}, I) \pi(\mathbf{T}, \mathbf{A} | I) d(\mathbf{T}, \mathbf{A}). \tag{7}$$

As $p(\mathbf{T}, \mathbf{A} | \mathbf{D}, I)$ of Eq. (6) cannot be represented in closed form due to the nonlinear nature of the model given in Eq. (2), it is convenient to form a compact representation based on $\mathbf{T}, \mathbf{A}$ [one example being the mean and/or covariance of $\mathbf{T}, \mathbf{A}$ as was done in Ref. 11]. In order to simplify the notation in the remainder of the paper, a compact representation will be denoted by

$$\begin{aligned} L &= \int f(\mathbf{T}, \mathbf{A}) p(\mathbf{T}, \mathbf{A} | \mathbf{D}, I) d(\mathbf{T}, \mathbf{A}) \\ &= \frac{1}{Z} \int f(\mathbf{T}, \mathbf{A}) l(\mathbf{T}, \mathbf{A} | \mathbf{D}, I) \pi(\mathbf{T}, \mathbf{A} | I) d(\mathbf{T}, \mathbf{A}), \end{aligned} \tag{8}$$

where $f(\mathbf{T}, \mathbf{A})$ of Eq. (8) is used to define a particular compact representation. Details of these compact representations (specifically the mean and covariance of $\mathbf{T}, \mathbf{A}$) using experimentally obtained data will be shown in Sec. V. In order to simplify the notation the authors combine the decay time and linear coefficients $\mathbf{T}, \mathbf{A}$ into a single parameter vector **X** when there is no need to distinguish between the two and the background information I is also dropped for the remainder of the paper for simplicity.

III. DIFFICULTIES WITH TWO COMMON MONTE CARLO ALGORITHMS

ISMC and MCMC algorithms both rely on choosing initial probability distributions representing the prior knowledge of the PPDF to be estimated. This section discusses potential difficulties in choosing these initial distributions. The initial distributions are denoted by either a *sampling distribution* for the ISMC algorithm or *proposal distribution* for the MCMC algorithm.

A. ISMC integration algorithms

The work by Xiang *et al.*[11] used ISMC integration in which the ISMC sampling distribution $g(\mathbf{X})$, with a support greater than $p(\mathbf{X}|\mathbf{D})$, is applied to the integral of Eq. (8) as follows:

$$L = \int f(\mathbf{X}) \frac{p(\mathbf{X}|\mathbf{D})}{g(\mathbf{X})} g(\mathbf{X}) d\mathbf{X} = \int f(\mathbf{X}) w(\mathbf{X}) g(\mathbf{X}) d\mathbf{X}, \quad (9)$$

with $w(\mathbf{X}) = p(\mathbf{X}|\mathbf{D})/g(\mathbf{X})$. The ISMC sampling distribution $g(\mathbf{X})$ can be effectively replaced with the approximation (see Appendix B)

$$\hat{g}(\mathbf{X}) = \frac{1}{M} \sum_{r=0}^{M-1} \delta(\mathbf{X} - \mathbf{X}_r), \quad (10)$$

where $\delta(\mathbf{X}-\mathbf{X}_r)$ is a Dirac delta function centered at the sample $\mathbf{X}_r$ drawn from the sampling distribution $g(\mathbf{X})$, and M is the number of such samples used. Using the approximation $\hat{g}(\mathbf{X})$ the representation of Eq. (9) is given by

$$L \approx \frac{1}{M} \sum_{r=0}^{M-1} \int f(\mathbf{X}) w(\mathbf{X}) \delta(\mathbf{X} - \mathbf{X}_r) d\mathbf{X}$$

$$= \frac{1}{M} \sum_{r=0}^{M-1} f(\mathbf{X}_r) w(\mathbf{X}_r). \quad (11)$$

The formalism of Eq. (11) using Eq. (10), termed ISMC integration, has been presented as opposed to defining "estimators" of L as is commonly found in statistical literature,[19] for the benefit of readers who are not well versed with statistical terminology.

The difficulty of choosing an appropriate ISMC sampling distribution $g(\mathbf{X})$ in high dimensions has been shown in Ref. 19. The difficulty can be demonstrated with an explicit numerical example (see Appendix C) to show that the difficulty still exists even in low dimensions. The following illustrative example shows how ISMC estimates can be very sensitive to poor choices of sampling distributions in terms of placement as well as variance. To highlight the difficulties, Fig. 1 illustrates a marginal PPDF $p(\mathbf{T}|\mathbf{D})$ evaluated for two different room impulse responses experimentally measured in real halls. Figure 1(a) shows a very sharply peaked PPDF while Fig. 1(b) shows a very narrow, elongated PPDF along one dimension. The ellipsoids marked in the figures conceptually indicate sampling distributions for ISMC. The ISMC sampling distribution marked by A, with a support greater than but similar to the actual PPDF $p(\mathbf{T}|\mathbf{D})$, is ideal for precise, unbiased estimations using ISMC integration. The ISMC sampling distribution B, with a support much greater than the actual PPDF $p(\mathbf{T}|\mathbf{D})$ still results in a reasonable ISMC integration estimate, but is less efficient as more samples will be required to obtain a good result. The ISMC sampling distribution C, with a support less than the actual PPDF $p(\mathbf{T}|\mathbf{D})$, will lead to failure of ISMC integration estimates as the variance of the estimates as given by Eq. (C2) will likely be unbounded. Figure 1 uses two actual PPDFs evaluated from experimentally measured results to demonstrate that a sampling distribution marked by A is in practice hardly possible without any prior knowledge on the sharpness (spreading), orientation, location, and size of actual PPDFs. In light of these difficulties, creating an efficient automated procedure for determining decay parameters and their reliability estimates from Schroeder decay curves using ISMC integration will be difficult, since the location of the PPDF mode, its shape, its orientation, and its size may not be known when the ISMC sampling distribution has to be selected.

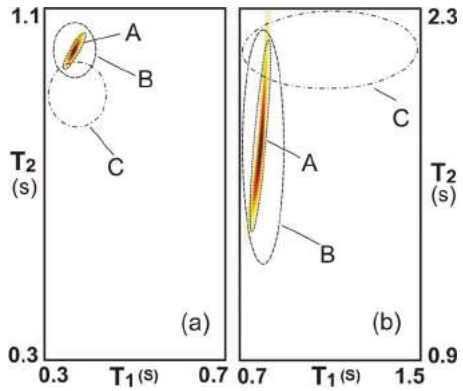

FIG. 1. (Color online) Marginalized PPDF $p(\mathbf{T}|\mathbf{D})$ evaluated for two different room impulse responses experimentally measured in real halls with ellipsoids indicating proposal distributions for ISMC integration. Proposal distributions marked by A, with support greater than the PPDF $p(\mathbf{T}|\mathbf{D})$, is ideal for precise, unbiased estimations using ISMC integration. Proposal distribution B, with a support greater than the PPDF $p(\mathbf{T}|\mathbf{D})$ still results in reasonable ISMC estimates, but is less efficient. Proposal distributions C, with a support less than the PPDF $p(\mathbf{T}|\mathbf{D})$, will lead to failure of ISMC estimates.

B. MCMC algorithms

An alternative to an ISMC integration approach is a MCMC algorithm such as the popular Metropolis–Hastings algorithm.[19] The Metropolis–Hastings algorithm generates *dependent* samples $\mathbf{X}_r$ from the PPDF $p(\mathbf{X}|\mathbf{D})$ using only knowledge of the likelihood and the prior $l(\mathbf{X}|\mathbf{D})\pi(\mathbf{X})$. As was done with the ISMC algorithm in Eq. (10), these samples can then be used to form an approximation of the PPDF $p(\mathbf{X}|\mathbf{D})$ by

$$p(\mathbf{X}|\mathbf{D}) \approx \frac{1}{M} \sum_{r=0}^{M-1} \delta(\mathbf{X} - \mathbf{X}_r), \quad (12)$$

which can estimate the representation of Eq. (8) by a Monte Carlo approximation

$$L \approx \frac{1}{M} \sum_{r=0}^{M-1} \int f(\mathbf{X}) \delta(\mathbf{X} - \mathbf{X}_r) d\mathbf{X} = \frac{1}{M} \sum_{r=0}^{M-1} f(\mathbf{X}_r). \quad (13)$$

The Metropolis–Hastings algorithm generates a sequence of samples $\mathbf{X}_r$ through the parameter space by a random walk. At each step of the algorithm a sample $\mathbf{S}_r$ in the parameter space is chosen with probability distribution given by $h(\mathbf{S}_r - \mathbf{X}_r)$, where $h(\mathbf{X})$ is a user defined proposal distribution. The sample $\mathbf{S}_r$ is accepted (i.e., $\mathbf{X}_{r+1} = \mathbf{S}_r$) with a probability

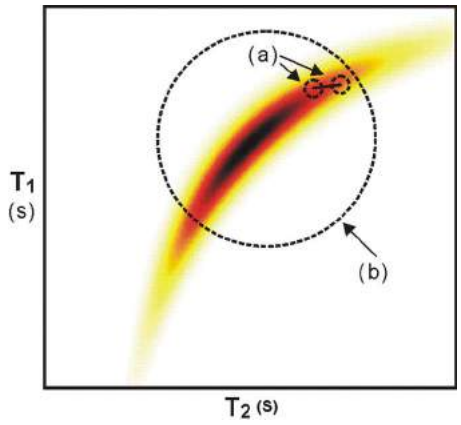

FIG. 2. (Color online) Example of potential problems in choosing a proposal distribution for the Metropolis–Hastings MCMC algorithm with symmetric normal proposal distribution. Circles show one standard deviation distance from the mean. (a) Small tailed proposal distribution $h(\mathbf{T})$ with too small support in comparison to the PPDF $p(\mathbf{T}|D)$ results in most of the proposed MCMC samples $\mathbf{S}_r$ being accepted but with a slow exploration of the PPDF $p(\mathbf{T}|D)$. (b) Heavy tailed proposal distribution with excessive support in comparison to the PPDF $p(\mathbf{T}|D)$ results in majority of the proposed MCMC samples $\mathbf{S}_r$ being rejected, which also results in a slow exploration of the PPDF $p(\mathbf{T}|D)$.

$$\min\left[1, \frac{p(\mathbf{S}_r|\mathbf{D})h(\mathbf{S}_r - \mathbf{X}_r)}{p(\mathbf{X}_r|\mathbf{D})h(\mathbf{X}_r - \mathbf{S}_r)}\right], \tag{14}$$

and rejected (i.e., $\mathbf{X}_{r+1}=\mathbf{X}_r$) otherwise. Both $p(\mathbf{S}_r|\mathbf{D})$ and $p(\mathbf{X}_r|\mathbf{D})$ of Eq. (14) are evaluated from the posterior distribution. The proposal distribution $h(\mathbf{X})$ is commonly chosen to be a symmetric function in which case $h(\mathbf{S}_r-\mathbf{X}_r)=h(\mathbf{X}_r-\mathbf{S}_r)$ and so Eq. (14) reduces to

$$\min\left[1, \frac{p(\mathbf{S}_r|\mathbf{D})}{p(\mathbf{X}_r|\mathbf{D})}\right] \tag{15}$$

[see Appendix D for details on the validity of the acceptance probability of Eq. (14)]. While the proposal distribution $h(\mathbf{X})$ is not explicitly present in Eq. (15), the choice of $h(\mathbf{X})$ will have a large impact on the efficiency of the Metropolis–Hastings algorithm. If $h(\mathbf{X})$ has much thicker tails than the PPDF $p(\mathbf{X}|\mathbf{D})$ then the acceptance probability of Eq. (15) will be very low for most of the proposed samples $\mathbf{S}_r$, which results in $\mathbf{X}_{r+1}=\mathbf{X}_r$ for most r, and so the algorithm will not explore the parameter space efficiently. Similarly if $h(\mathbf{X})$ has much thinner tails than the PPDF $p(\mathbf{X}|\mathbf{D})$ then $p(\mathbf{S}_r|\mathbf{D})/p(\mathbf{X}_r|\mathbf{D})\approx 1$ and so almost all of the proposed samples $\mathbf{S}_r$ will be accepted; however, the algorithm will still explore the parameter space very slowly as $p(\mathbf{X}_{r+1}|\mathbf{D})=p(\mathbf{S}_r|\mathbf{D})\approx p(\mathbf{X}_r|\mathbf{D})$. Figure 2 conceptually shows an example of two symmetric normal proposal distributions superimposed on two different PPDFs with dashed-line circles indicating a distance of one standard deviation from the mean. Figure 2(a) illustrates a thin tailed proposal distribution in comparison with the PPDF shown, which results in a slow exploration of the PPDF even though most of the proposed samples are accepted. Figure 2(b) shows a case where the proposal distribution has a thicker tail in one dimension than the PPDF, which will cause most of the proposed samples to be rejected, again resulting in a slow exploration of the PPDF.

IV. THE SLICE SAMPLING MONTE CARLO ALGORITHM

As shown in Sec. III, both the Metropolis–Hastings MCMC algorithm and the ISMC algorithm suffer from the requirement of a good initialization of proposal/sampling distributions. For efficiently determining the representation of Eq. (8) it is important to use an algorithm that is less dependent on good initialization than either the Metropolis–Hastings MCMC or ISMC integration algorithms. The SSMC algorithm as presented by Neal[13] was developed, in part, to minimize the effect of the proposal distributions on efficiency of the algorithm.

A. The SSMC algorithm

The fundamental principle of the SSMC algorithm is to introduce an auxiliary probability distribution, which will aid generating samples from the desired distribution. As an example consider a one-dimensional PPDF $p(X|\mathbf{D})$. One can define an auxiliary distribution[13] by

$$p(X,y|\mathbf{D}) = \begin{cases} 1 & \text{if } 0 < y < p(X|\mathbf{D}) \\ 0 & \text{otherwise.} \end{cases} \tag{16}$$

Marginalization over the variable y results in

$$\int p(X,y|\mathbf{D})dy = \int_0^{p(X|\mathbf{D})} 1dy = p(X|\mathbf{D}), \tag{17}$$

which is the desired posterior distribution. As in any Monte Carlo approach the marginalization can be implemented by sampling from the joint distribution $p(X,y|\mathbf{D})$ and ignoring the parameter y. The multidimensional PPDF $p(\mathbf{X},y|\mathbf{D})$ of Eq. (6) can be handled in the same manner by simply applying the auxiliary distribution of Eq. (16) to each component X_j individually

$$p(X_j,y|\mathbf{D}) = \begin{cases} 1 & \text{if } 0 < y < p(X_j|\mathbf{D}) \\ 0 & \text{otherwise,} \end{cases} \tag{18}$$

as is done in Gibbs sampling approach.[3,7,19] A key element of the SSMC algorithm is that it effectively replaces the sampling distribution (ISMC) or proposal distribution (MCMC) algorithms with a uniform proposal distribution; its spreading is adaptively constrained by the PPDF to be sampled. The principle benefit of this approach is that it allows for an adaptive tuning within the SSMC algorithm (which is difficult to achieve with other MCMC algorithms). This paper presents a simplified SSMC algorithm as discussed in Ref. 13, in which the adaptive tuning of the auxiliary variable is achieved using an interval doubling technique. Other more elaborate versions of the SSMC algorithm, as well as proofs of validity of the algorithm, are described in the original Ref. 13. As with the Metropolis–Hastings algorithm, the SSMC algorithm has a update rule, which defines a new sample $\mathbf{X}_{r+1}$ in the parameter space given the current sample $\mathbf{X}_r$. The authors present the simplified SSMC algorithm and update rule below.

Algorithm 1. Simplified slice sampling: Return sample X_{r+1} given sample X_r drawn from the distribution $p(X|\mathbf{D})$.

1: $y=a$ random value from uniform distribution $[0,p(X_r|\mathbf{D})]$
2: $u=a$ random value from uniform distribution [0,1]
3: $x_l=X_r-(1-u)w$
4: $x_r=X_r+uw$
5: **while** $p(x_l|\mathbf{D})\geq y$ **do**
6: $x_l=x_l-w$
7: **end while**
8: **while** $p(x_r|\mathbf{D})\leq y$ **do**
9: $x_r=x_r+w$
10: **end while**
11: **while** 1 **do**
12: $x'=a$ random value from uniform distribution $[x_l,x_r]$
13: **if** $p(x'|\mathbf{D})\geq y$ **then**
14: **return** $X_{r+1}=x'$
15: **else**
16: **if** $p(x'|\mathbf{D})\leq p(x_l|\mathbf{D})$ **then**
17: $x_l=x'$
18: **end if**
19: **if** $p(x'|\mathbf{D})\geq p(x_r|\mathbf{D})$ **then**
20: $x_r=x'$
21: **end if**
22: **end if**
23: **end while**

B. A graphical illustration of the SSMC algorithm

Figure 3(a) shows a unimodal marginal PPDF $p(X|\mathbf{D})$ with an initial starting sample given by X_0 and the value of y randomly chosen from the uniform distribution defined over $[0,p(X_0|\mathbf{D})]$, which corresponds to step 1 of Algorithm 1. Figure 3(b) shows the "slice" S of the parameter space defined as the region where $p(X|\mathbf{D})>y$. Figure 3(c) shows the random stepping out procedure of steps 3–10, which have been done through an interval doubling approach.[13] The result is that the bounding interval B contains the slice S. Figure 3(d) shows a randomly selected point X' chosen within the bounding interval B. As the point X' is not inside the slice S the bounding interval is shrunk to where the point X' defines a new boundary point [in this case the new value for x_l for the interval B' as is shown in Fig. 3(e) corresponds to steps 11–23 in Algorithm 1]. Finally, Fig. 3(f) shows a randomly selected point X'' drawn from B' also contained in the slice S. This point X'' is accepted as a new sample X_1. The process is then iterated with X_1 as the initial sample of the algorithm.

An important feature of the SSMC algorithm is that it generates samples relying only on a uniform proposal distribution whose variance is determined adaptively. In other words, SSMC can explore the PPDF efficiently by updating knowledge from the PPDF to be sampled while the sampling is in progress.

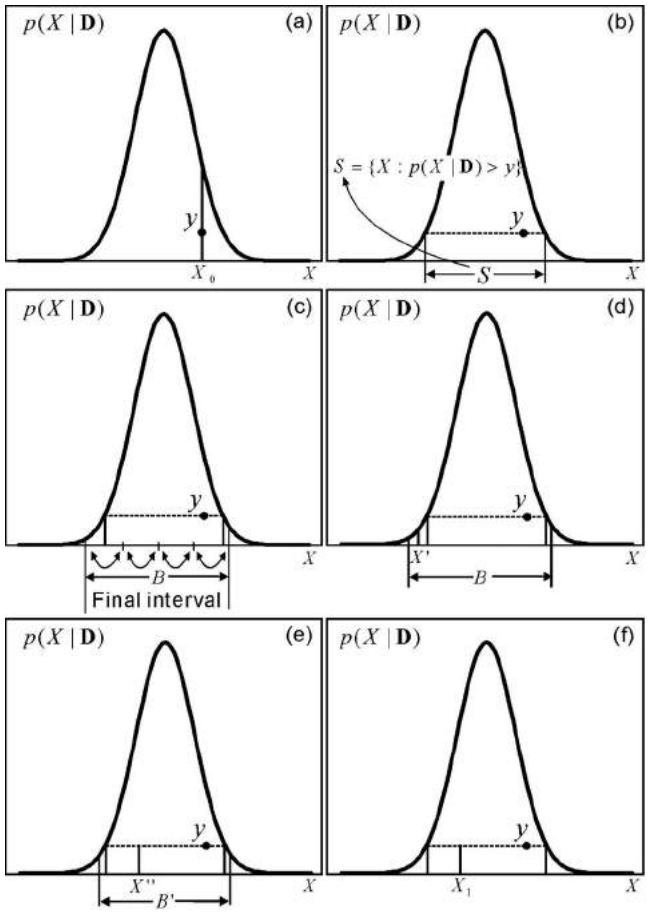

FIG. 3. Iterative steps of the slice sampling illustrated using an exemplary unimodal PPDF. One-dimensional parameter X is used for an illustrative discussion. For the experimental data discussed in Sec. V $X=A_j$ (with $j=0,1,2$) or $X=T_k$ (with $k=1,2$), respectively. (a) Unimodal PPDF $p(X|\mathbf{D})$ with an initial starting sample given by X_0 and the randomly chosen value of y, which corresponds to step 1 of Algorithm 1. (b) Slice S of the parameter space defined as the region where $p(X|\mathbf{D})>y$, namely, $S=\{X:p(X|\mathbf{D})>y\}$. (c) Random stepping out procedure of steps 3–10, which have been done through an interval doubling approach. (d) Randomly selected point X' chosen within the bounding interval B. As the point X' is not inside the slice S the bounding interval is shrunk to where the point X' defines a new boundary point [in this case the new value for x_l for the interval B' as is shown in (d) and corresponds to steps 11–23]. (e) Randomly selected point X'' drawn from B' also contained in the slice S. This point X'' is accepted as a new sample X_1. The process is then iterated with X_1 as the initial sample of the algorithm.

C. Initialization and convergence of the SSMC algorithm

The SSMC algorithm still requires the user to specify the interval doubling parameters w_{T_j} and w_{A_j}, where w_{T_j} and w_{A_j} correspond to the estimate of the spread of the PPDF $p(\mathbf{X}|\mathbf{D})$ in each of the T_j and A_j parameters, respectively. The choice of w_{T_j} can, in principle, be chosen fairly well based on the expected precision in architectural acoustics practice. In the practical implementation of SSMC, a rough estimation of the reverberation time, in case of a single-slope energy decay, can be easily deduced using a small early-decay portion of the decay function, while its standard deviation τ is expected about 1% of the reverberation time T to be determined, which leads to a proper choice of w_{T_j}. In case of a double-slope energy decay, the primary decay time T_1

can be easily estimated in the same way as for the reverberation time in the single-slope case, and the secondary decay time T_2 is expected to be larger than T_1 (see Ref. 2); however, the standard deviation τ_2 of T_2 is expected to be in the same order or even larger than τ_1 of T_1, which means a similar order of w_{T_1} and w_{T_2} can be straightforwardly chosen in the practical implementation of the SSMC algorithm in order to reach the expected precision in architectural acoustics practice. An important advantage of the SSMC algorithm over ISMC integration or conventional MCMC algorithms (such as Metropolis–Hastings) is that the w_{T_j} and w_{A_j} are adjusted dynamically by the algorithm, and so the SSMC algorithm is less sensitive to a poor choice of these values. In fact, w_{T_j} and w_{A_j} can be updated dynamically from sample to sample based on information gained during shrinking steps of the previous samples. This fact is especially beneficial as choosing values for the w_{A_j} parameters is more difficult than for w_{T_j} parameters and good rules of thumb are as of yet unknown. Section V will elaborate on the initialization of the interval doubling parameter $\mathbf{w}$ using experimentally measured data. As with all other MCMC algorithms the efficiency of the SSMC algorithm will depend on the initial starting sample $\mathbf{X}_0$. If the sample $\mathbf{X}_0$ is in a region of low PPDF values, the algorithm will take longer to converge to the PPDF and so many of the initial samples do not represent the PPDF well. This problem is often alleviated using a "burn-in" phase, in which sample $\mathbf{X}_0$ is chosen after a certain amount of initial samples $\mathbf{X}_{-m},\ldots,\mathbf{X}_{-1}$ are discarded. The burn-in phase of the algorithm can be avoided using the FS algorithm[12] to choose the initial sample $\mathbf{X}_0$ for both the linear $\mathbf{A}$ and decay time $\mathbf{T}$ parameters. The ability to choose the initial parameters $\mathbf{T}$ and $\mathbf{A}$ using the FS algorithm and the ability of the SSMC algorithm to overcome poor choices for w_{T_j} and w_{A_j} allows for a combined algorithm, which is especially useful in architectural acoustics practice. As with other MCMC algorithms, the dependent samples $\mathbf{X}_r$ generated by the SSMC algorithm can be used to approximate the representation of Eq. (8); however, proving when the calculated representation of Eq. (8) has converged is an open research problem (a problem shared by all MCMC and MC algorithms). Section V B discusses one particular heuristic method to detect convergence.

V. EXPERIMENTS

An intimate performance hall (Susan Howorth Theater) in Powerhouse Arts Center, Oxford, MS is coupled to a reverberant gallery. The gallery and the theater measures are $21.3\times12.2\times7.4$ m^3 and $21.3\times16.2\times7.63$ m^3, respectively (see a sketch in Fig. 4). With doors closed, the natural reverberation times averagely amount to 1.5 s for the primary space (theater) and 3.9 s for the secondary space (gallery), respectively. In the acoustically coupled-spaces, when the primary space possesses shorter nature reverberation times than the secondary space, energy decays often exhibit double-sloped decay behaviors.[2] To investigate the energy decay characteristics, an omni-directional sound source is placed at the middle of the stage, whereas an omni-directional microphone as a sound receiver is located at

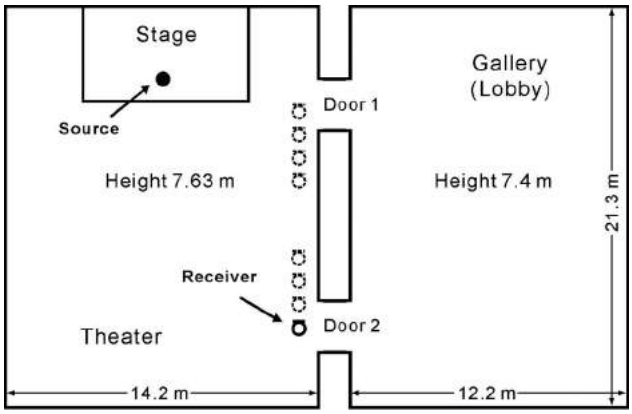

FIG. 4. Plane view of the Susan Howorth Theater in Powerhouse Arts Center, Oxford, MS. Two doors couple the theater and a reverberant gallery. Sound source is positioned on the stage, room impulse responses at receiver positions near two doors are measured, and the current paper focuses on one data set at the position marked by a solid-line symbol.

many strategic positions as indicated in sketch (Fig. 4). Room impulse responses are measured. In order to analyze decay characteristics over architectural acoustics-relevant frequency ranges, each room impulse response is first (octave) band-pass filtered. Schroeder integration is then applied to the room impulse responses for each octave band. A five-parameter model representing a double-slope decay associated with two decay times is used for energy decay analysis based on Schroeder integration results

$$F(t_k,\mathbf{T},\mathbf{A}) = A_0(t_K - t_k) + A_1\exp(-13.8t_k/T_1) + A_2\exp(-13.8t_k/T_2). \quad (19)$$

This model has exemplary illustrative purpose, as it is of both practical importance to architectural acousticians and sufficiently complex to demonstrate the benefits of the combined SSMC/FS algorithm in creating a method for estimating decay times with a minimum of user interaction. In the following the authors discuss the measurement results from a specific location being close to an opening door (door 2) to the gallery. The authors use exemplary data, which are a room impulse response band-pass filtered at 250 Hz octave band [see Fig. 5(a)] for the following discussion. Figure 5(b) illustrates the resulting Schroeder decay curve. The likelihood and posterior are determined as described in Sec. II, which results in a PPDF over a six-dimensional space when including variance σ^2 as a unknown parameter using Eq. (3), or with σ being removed by marginalization using Eq. (4) the PPDF is defined over a five-dimensional parameter space given by the decay times $\mathbf{T}$ and linear coefficients $\mathbf{A}$.

A. Initializing the SSMC/FS algorithm with experimental data

Applying the FS algorithm to the experimental data resulted in an initial estimate of both the decay time and linear parameters. The initial estimates $T_1=1.5$ s and $T_2=3.3$ s and $A_0=-4.0e-8$, $A_1=0.2486$, and $A_2=0.0613$, for a decay data segment starting −5 dB until the end of the decay trace [see Fig. 5(b)], are then used as the initial starting point of the SSMC algorithm. Decay time interval doubling values of

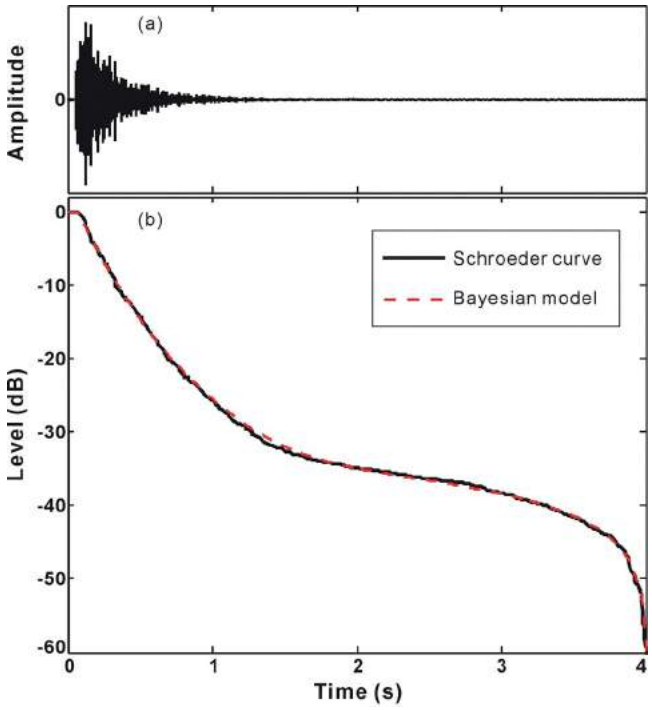

FIG. 5. (Color online) Room impulse response and corresponding decay curves experimentally measured in Howorth Theater. (a) Room impulse response after octave band-pass filtering. (b) Schroeder decay curve evaluated from the room impulse response compared with the Bayesian decay model curve determined by the SSMC/FS algorithm.

$w_{T_1}=0.03$ and $w_{T_2}=0.1$ are chosen based on the discussion given in Sec. IV C. Figures 6(c) and 6(e) show the marginal distributions of the decay time parameters T_1 and T_2 created from samples generated by the SSMC algorithm. The value of $w_{T_1}\approx 0.03$ is approximately three times that of the spread for T_1, while the value of $w_{T_2}\approx 0.1$ is a good guess to the spread of T_2. The linear coefficient doubling values are assigned values of $w_{A_0}=1$, $w_{A_1}=1$, and $w_{A_2}=1$. Figures 6(a), 6(b), and 6(d) show the marginal distributions of the linear parameters A_0, A_1, and A_2 created from samples generated by the SSMC algorithm. The values of w_{A_1} and w_{A_2} are approximately 30 times that of the spread for $A_1, A_2\approx 0.03$, while the value of w_{A_0} is approximately 3×10^6 times that of the spread for $A_0\approx 3\times 10^{-7}$. This poor choice of $w_{A_0}=1$, $w_{A_1}=1$, and $w_{A_2}=1$ represents a typical case in which an acoustician would have difficulty in assigning these parameters with good initial values. The SSMC algorithm, however, can compensate for this poor choice as will be shown in Sec. V B.

B. Convergence and decay parameter estimation for the experimental data

The SSMC algorithm is asymptotically guaranteed to converge and produce a sequence of M dependent samples $\mathbf{X}_0, \mathbf{X}_1, \ldots, \mathbf{X}_{M-1}$ from the PPDF $p(\mathbf{X}|\mathbf{D})$. There is, however, no indication as to how many samples are required to properly represent the PPDF in order to calculate the representation of Eq. (13). Convergence can be heuristically determined by finding the number of samples M such that all desired moments of Eq. (13) have converged within a predefined tolerance. For the experimental data the means and covariances of the decay times and linear parameters were used to assess convergence of the SSMC algorithm. Specifically the SSMC algorithm was deemed to converge when the quantities

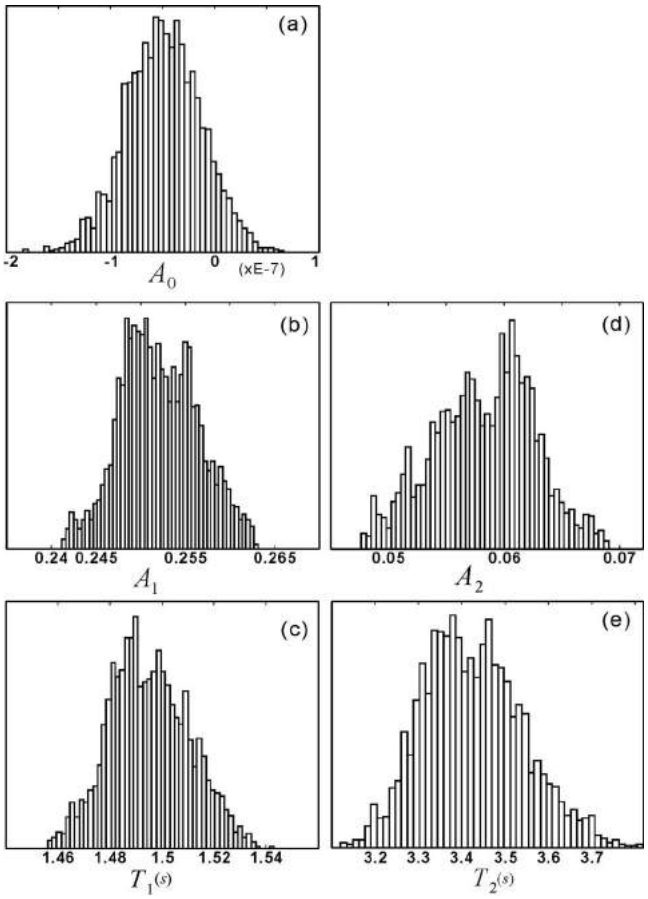

FIG. 6. Marginal histograms (MHs) of decay parameters from samples generated by SSMC/FS algorithm from experimental data measured in Susan Howorth Theater. (a) MH for A_0. (b) MH for A_1. (c) MH for T_1. (d) MH for A_2. (e) MH for T_2.

$$\langle \hat{X}_j \rangle = \frac{1}{M}\sum_{r=0}^{M-1} X_{j,r}, \tag{20}$$

$$\langle \hat{X}_{jk} \rangle = \frac{1}{M}\sum_{r=0}^{M-2} (X_{j,r} - \langle \hat{X}_j \rangle)(X_{k,r} - \langle \hat{X}_k \rangle) \tag{21}$$

change less than 0.1%, where X is any decay time T, or linear parameter A, and $X_{j,r}$ denotes the jth component of the rth sample. For the experimental data in Fig. 5, the SSMC/FS algorithm converged within ≈12 000 samples. It is useful in this context to provide the acousticians with the histogram outputs given in Fig. 6. As the likelihood function $l(\mathbf{X}|\mathbf{D})$ given by Eq. (4) is a student-T type distribution and the PPDF is given by $p(\mathbf{X}|\mathbf{D}) \propto l(\mathbf{X}|\mathbf{D})\pi(\mathbf{X})$, histograms which follow the shape of a student-T distribution provide added evidence that the SSMC/FS algorithm has converged.

The moment estimates of Eqs. (20) and (21) were then used as the decay parameter estimates once convergence was determined. Specifically for decay times, the mean

TABLE I. Decay parameters estimated from one measurement in the Susan Howorth Theater. Decay times (T_1 and T_2) along with their standard deviations (Std_1 and Std_2) derived from covariance matrix of slice sampling. Level difference defined by $\Delta L = 10\log(A_1/A_2)$, A_0 is used to estimate the peak-to-noise ratio (PNR) (Ref. 1). Cross-correlation coefficients (CCCs) are listed in the last column.

Band (Hz)	T_1 (s)	Std_1 (s)	T_2 (s)	Std_2 (s)	ΔL (dB)	PNR (dB)	CCC
125	1.83	5.55×10^{-2}	3.96	5.04×10^{-1}	17.3	64.3	0.79
250	1.47	1.65×10^{-2}	3.27	1.93×10^{-1}	5.73	54.9	0.83
500	1.48	5.88×10^{-2}	4.46	4.86×10^{-1}	12.75	49.1	0.77
1000	1.49	5.24×10^{-2}	5.15	7.67×10^{-1}	15.84	50.1	0.85
2000	1.32	2.36×10^{-2}	2.97	5.96×10^{-2}	13.46	52.0	0.78
4000	0.94	2.47×10^{-2}	2.61	3.93×10^{-1}	16.54	52.2	0.81

$$\langle \hat{T}_j \rangle = \frac{1}{M}\sum_{r=0}^{M-1} T_{j,r} \tag{22}$$

and covariance

$$\langle \hat{C}_{jk} \rangle = \frac{1}{M}\sum_{r=0}^{M-1} (T_{j,r} - \langle \hat{T}_j \rangle)(T_{k,r} - \langle \hat{T}_k \rangle) \tag{23}$$

(where $T_{j,r}$ denotes the jth decay time component of the rth sample) given the M samples used in assessing convergence were used as estimates of the decay times $\mathbf{T}$. From the expected covariance matrix $\langle \hat{\mathbf{C}} \rangle = [\langle \hat{C}_{jk} \rangle]$, the individual variances τ_j^2 and the standard deviation τ_j of each decay time T_j were estimated as discussed in Ref. 11. The expected standard deviation τ_j serves a reliability estimate, since it is a measure of "error bar" of the estimated decay time $\langle \hat{T}_j \rangle$, while the inter-relationship between the decay times is measured by cross-correlation coefficient (CCC) $\hat{C}_{jk}/\sqrt{\hat{C}_{jj}\hat{C}_{kk}}$.[11] The error bars and CCCs for the experimental example are listed in Table I.

For the linear parameters, the mean

$$\langle \hat{A}_j \rangle = \frac{1}{M}\sum_{r=0}^{M-1} A_{j,r} \tag{24}$$

and standard deviation

$$\text{Std}(\hat{A}_j) = \sqrt{\frac{1}{M}\sum_{r=0}^{M-1} (A_{j,r} - \langle \hat{A}_j \rangle)^2} \tag{25}$$

(where $A_{j,r}$ denotes the jth linear parameter component of the rth sample) given the M samples used in assessing convergence were used as estimates of the linear parameters $\mathbf{A}$. The means and standard deviations for the linear parameters for the experimental data taken at 250 Hz are shown in Table II. Figure 7 shows marginal posterior probability distributions (MPPDs) over two-dimensional (2D), zoomed-in parameter spaces from the experimental data. The MPPDs are generated by exhaustive sampling of the PPDF $p(\mathbf{X}|\mathbf{D})$ for all 2D MPPDs over $\{A_0,A_1\}$, $\{A_0,T_1\}$, $\{A_0,T_2\}$, $\{A_0,A_2\}$, $\{A_1,T_1\}$, $\{A_1,T_2\}$, $\{A_1,A_2\}$, $\{T_1,A_2\}$, $\{T_1,T_2\}$, and $\{A_2,T_2\}$, respectively. Parameters other than the pair shown were fixed to the mean values determined by Eq. (20) and given in Tables I and II. Estimated parameters listed in Tables I and II, when comparing with Fig. 7, indicate that the combined SSMC/FS algorithm successfully estimated the decay parameters and that the FS algorithm chose a good initial starting point for the SSMC algorithm. Figure 7 also shows that exhaustive sampling of the parameter space is not feasible without very good prior knowledge of the spread of the PPDF in all the dimensions. For example, exhaustive sampling over a five-dimensional space ranging between $-0.5e-7 \le A_0 \le 0.5e-7$, $0.1 \le A_1 \le 1.0$, $0.1 \le T_1 \le 5.0$, $0.001 \le A_2 \le 0.1$, and $1 \le T_2 \le 10$ (reasonable estimates of the parameter ranges for this acoustics problem), with each range partitioned into an appropriate number of cells to sample the marginal parameter distribution of Fig. 6, would require approximately 4×10^{12} samples compared to the 12 000 required for the SSMC/FS algorithm. Thus the SSMC/FS algorithm provides an efficient solution to the decay parameter estimation problem. Figure 7 also shows that choosing appropriate MCMC proposal or ISMC sampling distributions for the linear and decay time parameters can be difficult as there are large variations in sharpness (spreading) of the MPPDs, and in their orientations. While good MCMC proposal distributions could potentially be found by using initial runs or adaptive ISMC algorithms could be developed, in real experimental data, these variations also change from frequency band to frequency band, and from data to data, as such this task using ISMC or MCMC would be most likely require a significantly increased user tuning compared to the SSMC/FS algorithm.

TABLE II. Means (μ) and standard deviations (Std) of the linear parameters A_0, A_1, and A_2 estimated from the acoustical measurement in the Howorth Theater using the SSMC/FS algorithm, for 250 Hz octave-band evaluation.

Parameter	μ	Std
A_0	-2.91×10^{-8}	3.44×10^{-8}
A_1	0.2417	0.0044
A_2	0.0688	0.0044

It is unlikely that any type of initial processing used to define a MCMC proposal distribution and/or ISMC sampling distribution would not have an analog method to better choose the initial proposal distribution required by the SSMC algorithm as well, although this is a topic beyond the scope of the current work. Assessing SSMC convergence with the above heuristic scheme can be problematic for a PPDF with multiple modes or large areas with similar probability magnitude, where convergence of the representation will not give an indication that the SSMC algorithm has not

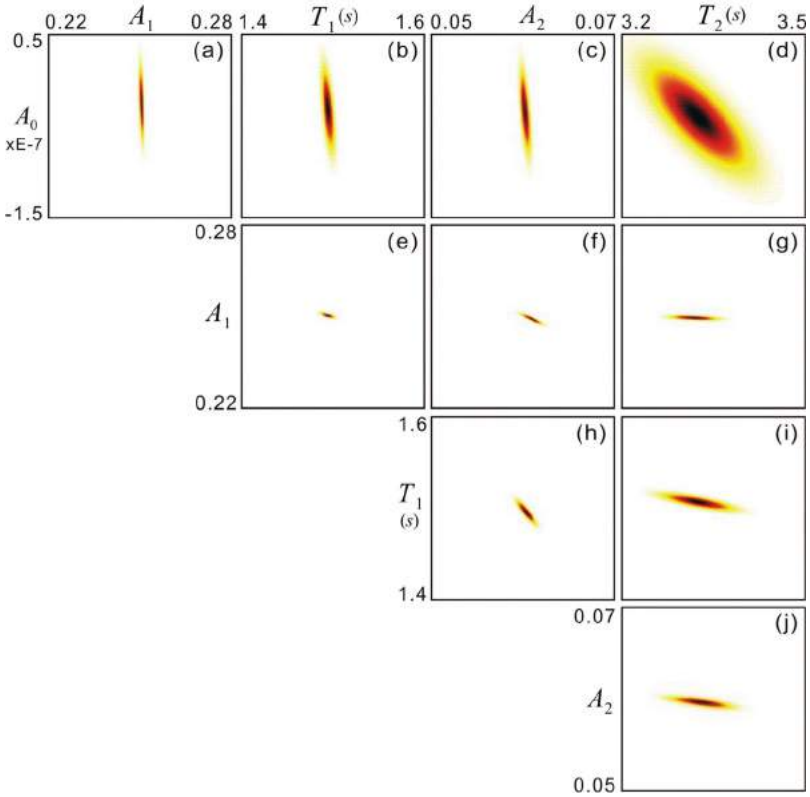

FIG. 7. (Color online) Marginal posterior probability distributions (MPPDs) over 2D (zoomed-in) parameter spaces from experimental data. Parameters other than the pair shown are fixed to the mean values (see Tables I and II). (a) MPPD over $\{A_0,A_1\}$. (b) MPPD over $\{A_0,T_1\}$. (c) MPPD over $\{A_0,A_2\}$. (d) MPPD over $\{A_0,T_2\}$. (e) MPPD over $\{A_1,T_1\}$. (f) MPPD over $\{A_1,T_2\}$. (f) MPPD over $\{A_1,T_2\}$. (g) MPPD over $\{T_1,A_2\}$. (h) MPPD over $\{T_1,A_2\}$. (i) MPPD over $\{T_1,T_2\}$. (j) $\{A_2,T_2\}$.

sufficiently explored the PPDF $p(\mathbf{X}|\mathbf{D})$. As discussed in Sec. IV, however, it is possible to focus on one mode of the PPDF; combining this fact with the use of the FS algorithm to initialize the SSMC algorithm in a region were the PPDF $p(\mathbf{X}|\mathbf{D})$ is significant allows for this heuristic scheme to be useful in practice. As assessing the convergence of MCMC and ISMC algorithms is also an open problem, the heuristic scheme discussed here is not considered as a drawback of the SSMC/FS algorithm in comparison to those algorithms.

VI. SUMMARY

This paper has shown that the SSMC algorithm is a suitable method for helping to automate the process of determining the decay parameter estimates in acoustically coupled-spaces with a minimum of user interaction and tuning. This paper has discussed potential problems with defining ISMC sampling distributions and MCMC proposal distributions when there was limited prior knowledge of the sharpness/position and orientation of the PPDF. In order to overcome this difficulty the SSMC algorithm was introduced in Sec. IV. The SSMC algorithm can overcome poor initialization of the proposal distribution through an adaptive process. In addition, Sec. IV also discussed how the FS algorithm could be combined with the SSMC algorithm to further improve SSMC performance by ignoring the burn-in phase and also improving the assessment of convergence for the SSMC algorithm. The SSMC/FS algorithm is applied to experimental data measured in Susan Howorth Theater in Sec. V. The plots of the MPPDs shown in Fig. 7 and the results in Tables I and II have demonstrated that the SSMC/FS algorithm is successful in estimating the decay parameters in an efficient manner as the number of samples required is on eight orders of fewer samples than possible through a deterministic exhaustive search algorithm, even with a relatively poor choice of initialization parameters. Figure 7 also illustrates the difficulty of defining ISMC sampling and MCMC proposal distributions for experimental data with a minimum of user tuning, which is especially important to acousticians who are unfamiliar with MCMC and ISMC algorithms, since large variations of posterior probability distributions in sharpness, orientation, position, and size can be encountered in the practice from data to data. A heuristic approach to assessing convergence of the SSMC/FS algorithm is also discussed. Choosing better heuristics specifically geared toward specific acoustics applications is an open problem not discussed in this paper.

In conclusion, the SSMC/FS algorithm is efficient in problems where good initialization of ISMC or MCMC algorithms is difficult, although it is possible that estimation of decay parameters in acoustically coupled-spaces (and other acoustics problems) could also be accomplished with a similar efficiency with better prior information about the nature of the PPDF and/or better expertise with MCMC and ISMC algorithms.

ACKNOWLEDGMENTS

The authors are very grateful to the reviewers for their insightful comments on the early version of the manuscript, which lead to a significant improvement of the paper. The authors would also like to thank David Woolworth for the data collection in the performance spaces. This paper is dedicated to Professor Jens Blauert on the occasion of his 70th birthday.

APPENDIX A

Marginalizing the likelihood given by Eq. (3)

$$l(\mathbf{T},\mathbf{A},\sigma|\mathbf{D},I) = (\sqrt{2\pi}\sigma)^{-K}\exp\left(\frac{-\mathbf{e}^{\mathrm{Tr}}\mathbf{e}}{2\sigma^2}\right) \tag{A1}$$

over the standard deviation σ can be accomplished by integrating the $l(\mathbf{T},\mathbf{A},\sigma|\mathbf{D},I)$ over σ using Jeffress' prior[18] $1/\sigma$, which results in

$$l(\mathbf{T},\mathbf{A}|\mathbf{D},I) = \int_0^\infty (\sqrt{2\pi}\sigma)^{-K}\exp\left(-\frac{Q}{\sigma^2}\right)\frac{1}{\sigma}d\sigma, \tag{A2}$$

where $Q=\mathbf{e}^{\mathrm{Tr}}\mathbf{e}/2$, then the identity[1]

$$\int_0^\infty x^{2n}\exp(-Qx^2)dx = \Gamma(n+1/2)\frac{Q^{-(n+1/2)}}{2} \tag{A3}$$

implies that

$$l(\mathbf{T},\mathbf{A}|\mathbf{D},I) = (2\pi)^{-K/2}\Gamma\left(\frac{K}{2}\right)\frac{Q^{-K/2}}{2}, \tag{A4}$$

which is Eq. (4).

APPENDIX B

Consider the PDF $g(\mathbf{X})$ and the cumulative density function (CDF) $G(\mathbf{X})$ related by

$$G(\mathbf{X}) = \int_{-\infty}^{\mathbf{X}} g(\mathbf{S})d\mathbf{S}, \tag{B1a}$$

$$g(\mathbf{X}) = \frac{d}{d\mathbf{X}}G(\mathbf{X}). \tag{B1b}$$

The representation of Eq. (9) can be determined using either the PDF or the CDF

$$L = \int f(\mathbf{X})w(\mathbf{X})g(\mathbf{X})d\mathbf{X} = \int f(\mathbf{X})w(\mathbf{X})dG(\mathbf{X}), \tag{B2}$$

where the CDF representation allows for both continuous and discrete distributions. The stepwise approximation

$$G(\mathbf{X}) \approx \frac{1}{M}\sum_{r=1}^{M} u(\mathbf{X}-\mathbf{X}_r), \tag{B3}$$

where $u(\mathbf{X})$ is a unit step function

$$u(\mathbf{X}) = \begin{cases} 1 & \text{if } \mathbf{X} \geq 0 \\ 0 & \text{otherwise}, \end{cases} \tag{B4}$$

is equivalent to creating a discrete or sampled approximation of the continuous CDF $G(\mathbf{X})$. Thus the representation of Eq. (9) is approximated by the sampled or discrete form of $G(\mathbf{X})$ as follows:

$$L \approx \frac{1}{M}\sum_{r=1}^{M}\int f(\mathbf{X})w(\mathbf{X})du(\mathbf{X}-\mathbf{X}_r). \tag{B5}$$

Using Eqs. (B1b) and (B3) and the property $\delta(\mathbf{X}-\mathbf{X}_r) = (d/d\mathbf{X})u(\mathbf{X}-\mathbf{X}_r)$ the approximated representation in Eq. (B5) can again be written with respect to the PDF $g(\mathbf{X})$. This results in Eq. (10) as follows:

$$g(\mathbf{X}) \approx \frac{1}{M}\sum_{r=1}^{M}\delta(\mathbf{X}-\mathbf{X}_r). \tag{B6}$$

TABLE III. Required number of samples M of the importance sampling for $3\sigma_w/\sqrt{M}<0.01$ given the absolute mean $|\mu|$ of the proposal distribution.

$\lvert\mu\rvert$	M
1	$1.55\times10^{+5}$
2	$4.83\times10^{+6}$
5	$6.49\times10^{+15}$

APPENDIX C

The following example illustrates the difficulties of choosing an importance sampling distribution (ISD) $g(X)$ in low dimensions. When generating independent samples from $g(X)$ is possible, the accuracy of the approximating representation is given by the central limit theorem[19]

$$|L_M - L| \to N\left(0,\frac{\sigma_w}{\sqrt{M}}\right) \quad \text{as } M\to\infty, \tag{C1}$$

where $N(\mu,\sigma)$ is a normal distribution with mean μ and standard deviation σ, with

$$\sigma_w^2 = \int \frac{(f(X)p(X))^2}{w(X)}dX - (L)^2. \tag{C2}$$

Consider the estimation of the normalizing constant

$$Z = \int \frac{p(X)}{g(X)}g(X)dX \tag{C3}$$

of a one-dimensional normal distribution with an unknown mean μ and identity standard deviation. The ISD is a zero-mean, normal distribution with an identity standard deviation. Using Eq. (C2), one can find the variance of the estimate as a function of μ given by

$$\sigma_w^2(\mu) = \exp(\mu^2) - 1. \tag{C4}$$

Table III shows the number of samples M required to achieve a standard statistical accuracy of $3\sigma_w/\sqrt{M}<0.01$ (a statistical 99.7% confidence interval that the result is correct) for different values of $|\mu|$. It is clear that the computational load required for the chosen ISD $g(X)$ becomes infeasible as $|\mu|$ increases.

APPENDIX D

This appendix presents a heuristic explanation of the acceptance probability given in Eq. (15) shown in Sec. III. For simplicity, the authors consider symmetric MCMC proposal distributions and a discrete parameter space. A MCMC transition kernel $K(\mathbf{X},\mathbf{U})=h(\mathbf{X}-\mathbf{U})$ defined by a symmetric proposal distribution $h(\mathbf{X}-\mathbf{U})=h(\mathbf{U}-\mathbf{X})$ [as is shown in Fig. 2, for example] represents the probability of moving from one point $\mathbf{X}$ in the parameter space to another $\mathbf{U}$. One must design the MCMC kernel $K(\mathbf{X},\mathbf{U})$ such that $p(\mathbf{X})$ (the distri-

bution of interest) is the unique invariant distribution of the kernel (see Ref. 19 for complete discussion of Markov chains and MCMC). The detailed balance property

$$h(\mathbf{X}-\mathbf{U})p(\mathbf{X}) = h(\mathbf{U}-\mathbf{X})p(\mathbf{U}) \tag{D1}$$

allows for $p(\mathbf{X})$ to be the desired invariance distribution. Thus detailed balance with a symmetric kernel implies that

$$p(\mathbf{X}) = p(\mathbf{U}) \tag{D2}$$

and so $p(\mathbf{X})$ is the uniform distribution. In order to generate samples from the desired invariant distribution $p(\mathbf{X})$, the MCMC transition kernel must be modified by the addition of an acceptance probability $A(\mathbf{X},\mathbf{U})$, which determines when a move from a point $\mathbf{X}$ to a proposed point $\mathbf{U}$ generated from the kernel $K(\mathbf{X},\mathbf{U})$ is accepted. Adding the acceptance probability, the detailed balance property becomes

$$A(\mathbf{X},\mathbf{U})h(\mathbf{X}-\mathbf{U})p(\mathbf{X}) = A(\mathbf{U},\mathbf{X})h(\mathbf{U}-\mathbf{X})p(\mathbf{U}) \tag{D3}$$

and so

$$A(\mathbf{X},\mathbf{U})p(\mathbf{U}) = A(\mathbf{U},\mathbf{X})p(\mathbf{X}). \tag{D4}$$

Choosing the acceptance probability $A(\mathbf{X},\mathbf{U}),A(\mathbf{U},\mathbf{X})$ so that $0 \le A(\mathbf{X},\mathbf{U}),A(\mathbf{U},\mathbf{X}) \le 1$ and satisfying the constraint given by Eq. (D4) result in $A(\mathbf{X},\mathbf{U})[p(\mathbf{X})/p(\mathbf{U})] \le 1$ and so $A(\mathbf{X},\mathbf{U}) \le [p(\mathbf{U})/p(\mathbf{X})]$. Thus setting $A(\mathbf{X},\mathbf{U}) = 1$ when $p(\mathbf{U}) \ge p(\mathbf{X})$ results in the proposed move $\mathbf{U}$ with higher probability always being accepted. Otherwise the proposed move $\mathbf{U}$ is accepted with probability $A(\mathbf{X},\mathbf{U}) = p(\mathbf{U})/p(\mathbf{X})$. This results in the acceptance probability for the MCMC algorithm given by

$$A(\mathbf{X},\mathbf{U}) = \min\left(1, \frac{p(\mathbf{U})}{p(\mathbf{X})}\right). \tag{D5}$$

It is important to note that the details of the symmetric proposal distribution $h(\mathbf{X}-\mathbf{U})$ do not effect the ability of the MCMC algorithm to correctly sample the desired distribution $p(\mathbf{X})$; however, the efficiency of the sampling is greatly dependent on the choice of the proposal distribution used (discussed in Sec. III).

[1]N. Xiang and P. M. Goggans, "Evaluation of decay times in coupled spaces: Bayesian parameter estimation," J. Acoust. Soc. Am. **110**, 1415–1424 (2001).

[2]N. Xiang and P. M. Goggans, "Evaluation of decay times in coupled spaces: Bayesian decay model selection," J. Acoust. Soc. Am. **113**, 2685–2697 (2003).

[3]S. Dosso, "Quantifying uncertainty in geoacoustic inversion. I. A fast Gibbs sampler approach," J. Acoust. Soc. Am. **111**, 129–142 (2002).

[4]J. Dettmer, S. E. Dosso, and Ch. W. Holland, "Model selection and Bayesian inference for high-resolution seabed reflection inversion," J. Acoust. Soc. Am. **125**, 706–716 (2009).

[5]S. E. Dosso and M. J. Wilmut, "Comparison of focalization and marginalization for Bayesian tracking in an uncertain ocean environment," J. Acoust. Soc. Am. **125**, 717–722 (2009).

[6]C.-F. Huang, P. Gerstoft, and W. S. Hodgkiss, "Statistical estimation of source location in presence of geoacoustic inversion uncertainty," J. Acoust. Soc. Am. **125**, EL171–176 (2009).

[7]Z. H. Michalopoulou and M. Picarelli, "Gibbs sampling for time-delay and amplitude estimation in underwater acoustics," J. Acoust. Soc. Am. **117**, 799–808 (2005).

[8]Z. H. Michalopoulou, "Multiple source localization using a maximum a posteriori Gibbs sampling approach," J. Acoust. Soc. Am. **120**, 2627–2634 (2006).

[9]Ch. Laplanche, "A Bayesian method to estimate the depth and the range of phonating sperm whales using a single hydrophone," J. Acoust. Soc. Am. **121**, 1519–1528 (2007).

[10]M. R. Schroeder, "New method of measuring reverberation time," J. Acoust. Soc. Am. **37**, 409–412 (1965).

[11]N. Xiang, P. M. Goggans, T. Jasa, and M. Kleiner, "Evaluation of decay times in coupled spaces: Reliability analysis of Bayesian decay time estimation," J. Acoust. Soc. Am. **117**, 3705–3715 (2005).

[12]N. Xiang and T. Jasa, "Evaluation of decay times in coupled spaces: An efficient search algorithm within the Bayesian framework," J. Acoust. Soc. Am. **120**, 3744–3749 (2006).

[13]R. M. Neal, "Slice sampling," Ann. Stat. **31**, 705–767 (2003).

[14]J. E. Summers, R. R. Torres, Y. Shimizu, and B.-I. L. Dalenbäck, "Adapting a randomized beam-axis-tracing algorithm to modeling of coupled rooms via late-part ray tracing," J. Acoust. Soc. Am. **118**, 1491–1502 (2005).

[15]D. T. Bradley and L. M. Wang, "The effects of simple coupled volume geometry on the objective and subjective results from nonexponential decay," J. Acoust. Soc. Am. **118**, 1480–1490 (2005).

[16]A. Billon, V. Valeau, A. Sakout, and J. Picaut, "On the use of a diffusion model for acoustically coupled rooms," J. Acoust. Soc. Am. **120**, 2043–2054 (2006).

[17]M. Meissner, "Computational studies of steady-state sound field and reverberant sound decay in a system of two coupled rooms," Cent. Eur. J. Phys. **5**, 293–312 (2007).

[18]E. T. Jaynes, *Probability Theory: The Logic of Science* (Cambridge University Press, Cambridge, 2003).

[19]C. C. Robert and G. Casella, *Monte Carlo Statistical Methods* (Springer-Verlag, New York, 1999).